Lithospheric structure of the Gorringe Bank: Insights into its origin and tectonic evolution

I. Jiménez-Munt,[1] M. Fernàndez,[1] J. Vergés,[1] J. C. Afonso,[1,2] D. Garcia-Castellanos,[1] and J. Fullea[1,3]

Received 4 February 2009; revised 11 March 2010; accepted 7 June 2010; published 29 October 2010.

[1] The Gorringe Bank is a 5000 m high seamount near the Atlantic coast of Iberia characterized by a 9 m high geoid anomaly and a ~120 mGal Bouguer anomaly relative to the surrounding abyssal plains. It has been linked to a NW directed thrust carrying exhumed upper mantle rocks and transitional crust on top of flexed-down Eurasian oceanic crust along the Tagus Abyssal Plain. However, estimations of crustal shortening have yielded dissimilar results, and the deep structure of the ridge remains highly unknown. We present a restored cross section and a new model of the lithospheric structure based on gravity, geoid, elevation, and the presence of serpentinized peridotites. At least 20 km of shortening took place along a flat-ramp-flat thrust fault, and the density structure of the lithosphere is consistent with mantle serpentinization varying from 70% at the surface to 20% at 14 km depth and 0% at 40 km. The topographic relief and gravity anomalies are explained by assuming a flexural isostatic model with an elastic thickness T_e of ~30 km. The evolution of the Gorringe Bank since the Late Jurassic is interpreted in relation to Eurasia-Africa-North America plate motion in four stages: (1) transtension between Newfoundland-Iberia and Africa, which generated small oceanic basins and mantle exhumation; (2) opening of the North Atlantic and seafloor spreading at the NW side of the exhumed Gorringe, which produced gabbro intrusions and serpentinization; (3) a quiescent tectonic period dominated by subsidence and sediment accumulation; and (4) a transpressional plate boundary between Eurasia and Africa with NW directed subcrustal thrusting and generation of the present Gorringe relief. **Citation:** Jiménez-Munt, I., M. Fernàndez, J. Vergés, J. C. Afonso, D. Garcia-Castellanos, and J. Fullea (2010), Lithospheric structure of the Gorringe Bank: Insights into its origin and tectonic evolution, *Tectonics*, *29*, TC5019, doi:10.1029/2009TC002458.

[1]Group of Dynamics of the Lithosphere, Institute of Earth Sciences Jaume Almera, CSIC, Barcelona, Spain.
[2]Now at ARC National Key Centre for Geochemical Evolution and Metallogeny of Continents, Department of Earth and Planetary Sciences, Macquarie University, Sydney, New South Wales, Australia.
[3]Now at Geophysics Section, School of Cosmic Physics, Dublin Institute for Advanced Studies, Dublin, Ireland.

0278-7407/10/2009TC002458

1. Introduction

[2] The Gorringe Bank is the most prominent topographic high, located westward of the West Iberian Margin, with a length of ~200 km in the ENE-WSW direction and a width of 80 km [*Auzende et al.*, 1984]. This seamount exhibits a high topographic relief of ~5000 m with respect to the surrounding Tagus Abyssal Plain, with its peak (Mount Gettysburg) at only ~24 m below sea level [*Auzende et al.*, 1984; *Girardeau et al.*, 1998] (open white triangle in Figure 1). The gravity field shows a 9 m positive anomaly in the geoid and a 120 mGal positive Bouguer anomaly, undoubtedly associated with the Gorringe Bank.

[3] Dredging campaigns have revealed that the summit of the Gorringe Bank is composed mainly of peridotites, gabbros, and less abundant extrusive rocks [*Auzende et al.*, 1984] (GORRINGE cruise 1996 [e.g., *Girardeau et al.*, 1998]). The surrounding seismic stratigraphy and shallow structure are established from several seismic surveys in the region in combination with Deep Sea Drilling Projects (DSDPs) 120 and 135 (Figure 1). According to *Girardeau et al.* [1998], the Gorringe Bank corresponds to a massive exhumed mantle ridge of highly serpentinized peridotite enclosing a 500 m thick gabbro layer, locally cut and partly covered by tholeiitic rocks. The rock assemblage would have formed at an oceanic ultraslow, cold, accreting center. These rocks were exhumed by passive tectonic denudation of the lithospheric mantle and associated crustal rocks during an amagmatic stretching episode that followed a magmatic one. The deep structure of the Gorringe Bank is not well imaged from the available seismic data in terms of either its internal geometry or its velocity distribution. Available wide-angle seismic data in the Tagus and Horseshoe abyssal plains show anomalous velocity-depth profiles that have been interpreted as ocean-continent transitional crust evolving to oceanic crust seaward [e.g., *Purdy*, 1975; *Pinheiro et al.*, 1992; *Afilhado et al.*, 2008]. Therefore, current crustal models of the Gorringe Bank are based on numerical modeling of geophysical observables, namely, gravity, geoid, elevation, magnetics, and their combinations.

[4] The first interpretations were published in the early 1970s by *Le Pichon et al.* [1970] and *Purdy* [1975], who interpreted the Gorringe Bank as an incipient subduction zone with Africa overriding the Eurasian plate and the crust and upper mantle involved in the overriding block. *Souriau* [1984] modeled the measured gravity and geoid anomalies and found that they could be explained by a 60 km deep-seated low-density body in the upper mantle. Although there was a good geometrical fit to the proposed model, it was difficult to explain in terms of petrology. *Mauffret et al.*

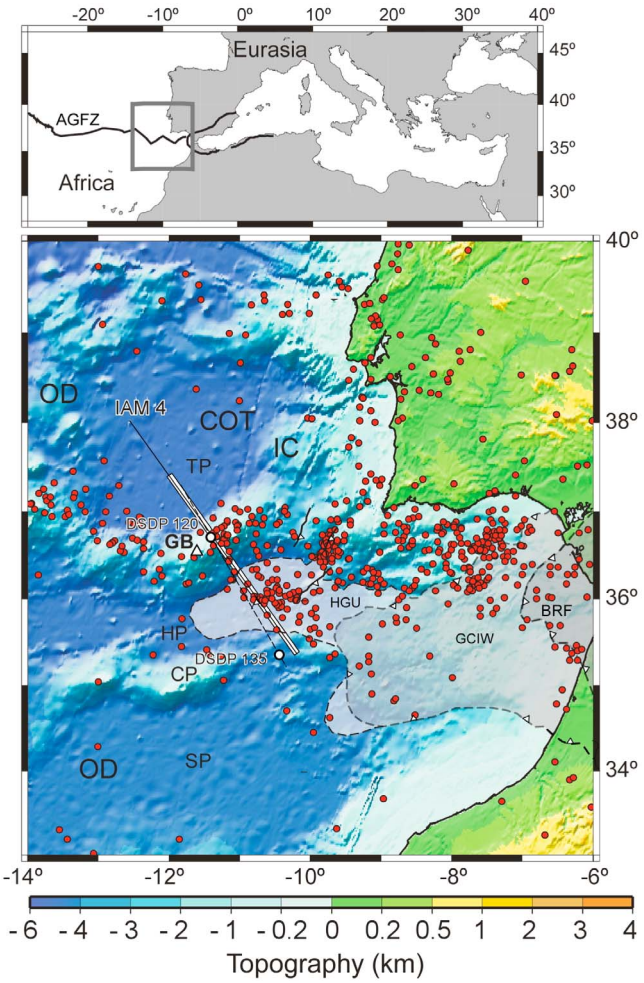

Figure 1. Topography of the study region with localization of deep seismic profiles (IAM-4 as solid line [*Banda et al.*, 1995], and AR92-3 as dashed line [*Sartori et al.*, 1994]) and our modeled transect (open white box). The modeled profile is in the NW-SE direction, from Tagus Abyssal Plain (TP) crossing the Gorringe Bank (GB) and Horseshoe Abyssal Plain (HP). Different domains according to *Rovere et al.* [2004]. OD, Oceanic domain; COT, Continent-ocean transition; IC, Iberian Continental domain; CP, Coral Patch Seamount; SP, Seine Abyssal Plain; GCIW, Gulf of Cadiz Imbricate Wedge; BRF, Betic-Rif Front; HGU, Horseshoe Gravitational Unit [*Iribarren et al.*, 2007]. Red circles indicate earthquakes with magnitude greater than 3.5 (data taken from Instituto Geográfico Nacional, Spain, http://www.ign.es/).

[1989] interpreted the flexure of the Tagus Abyssal Plain as evidence for thrusting of the Gorringe Bank above it. On the basis of 3-D gravity modeling, *Bergeron and Bonnin* [1991] proposed that the topographic highs are related to a shallow Moho and thus not isostatically supported. *Sartori et al.* [1994] used results from the AR92-3 deep seismic survey to propose folding of the Gorringe Bank above a high-angle fault flattening down and soling out at the base of the crust. In their interpretation, the Gorringe Bank would be uplifted 4–5 km above regional. Using collected samples from the Gorringe Bank, *Girardeau et al.* [1998] proposed that its present altitude is due to isostatic upward movement caused by serpentinization of upper mantle peridotites. *Hayward et al.* [1999] modified the broken plate model suggested by *Mauffret et al.* [1989] and used gravity observations to conclude that an elastic thickness of 35 km is needed in addition to 50 km of tectonic displacement of the Gorringe Bank above the Tagus Abyssal Plain to fit the observables. Some recent papers suggested that the Gorringe Bank may be a large pop-up structure by proposing a back thrust along its SE flank combined with a fore thrust along its NW flank [e.g., *Tortella et al.*, 1997]. On the basis of their interpretation of gravity and magnetic data, *Galindo-Zaldívar et al.* [2003] suggested that the Gorringe Ridge is the result of a NW verging planar low-angle thrust at crustal scale involving lower crust modified by the intrusion of lenses of gabbros and peridotites derived from the upper mantle. Estimates of shortening based on the geometry of the obtained models range between a minimum of 20 km [*Galindo-Zaldívar et al.*, 2003] and a maximum of 50 km [*Hayward et al.*, 1999]. However, no depth-converted balanced cross section of the Gorringe Bank has been reported. Finally, *Conti et al.* [2004] found shallow water fossils of 145–155 Ma at the summit of the ridge, suggesting that the Gorringe was a seamount at the early opening of the Atlantic. These authors interpreted the Gorringe as corresponding to a transverse ridge and proposed that it remained at shallow water depths from its formation to the present.

[5] In summary, the numerous interpretations proposed so far to explain the deep structure of the Gorringe Bank can be grouped into three end member categories: (1) shallow Moho and upward bending of the crust, (2) flat Moho and crustal thickening by thrusting, and (3) overthrusting of a broken plate with a Moho discontinuity. Presently, there is a general consensus that the Gorringe is a compressive structure located at the boundary between the Eurasian and African plates and that its prominent topographic relief is supported by flexural isostasy. Models based on local isostasy require a deep subvertical low-density body that produces the dynamic topography, which is difficult to reconcile with observations [*Souriau*, 1984]. Interestingly, all published models can reproduce some of the geophysical observables, and thus the models appear to be indistinguishable by potential fields only.

[6] The mechanism of mantle exhumation has been related to either rifting and low-angle extensional detachments or to upright tectonics in a transverse ridge setting as proposed by *Bonatti* [1978] to explain the presence of ridges in oceanic fracture zones. Similarly, whether serpentinized peridotites form a massive body or are small lenses interbedded within uplifted lower crust is also controversial. A highly debated question is the relationship between the Gorringe Bank and the Eurasia-Africa-North America plate boundaries and the origins of its present crustal and lithospheric structure. Most models suggest that the proto-Gorringe Bank was a portion of the E-W Eurasian-African plate boundary dominated by a strike-slip or weakly transtensive tectonic regime, which was subsequently reoriented NE-SW during the African-Eurasian convergence. However, this scenario does not easily match

the mantle exhumation required to form a massive peridotite ridge [*Girardeau et al.*, 1998] and neglects the interaction between this segment of the plate boundary and the subsequent opening of the northern segment of the Atlantic Ocean [e.g., *Le Gall et al.*, 1997].

[7] All these open questions cannot be solved independently, and thus we present an integrated study that fits with current work in the region and attempts (1) to establish the deep structure of the Gorringe Bank on the basis of available geological and geophysical data and (2) to find a formation mechanism for the Gorringe Bank compatible with petrological data, the large-scale plate tectonic setting, and the present-day deep structure.

[8] To address these questions, we first present a depth-converted balanced cross section of the Gorringe Bank as well as a restored version during the Late Cretaceous to present based on available multichannel seismic data that permits evaluation of crustal shortening. Second, we model the present-day lithospheric structure of the Gorringe Bank, integrating gravity, geoid, surface heat flow, and elevation data and considering flexural isostasy and geological and petrological data. Finally, the obtained results are discussed in terms of a possible evolutionary model of the Gorringe Bank since the Late Jurassic, which is supported by large-scale kinematic plate reconstructions.

2. Tectonic Setting

[9] The Eurasian-African plate boundary between the Azores triple junction and the Gibraltar Strait is characterized by a complex tectonic regime, varying from transtensive in the west to transpressive in the east, with strike-slip motion in its central segment (Figure 1). Seismic data and numerical modeling reveal that the plate boundary is relatively narrow to the west of the Gorringe Bank, whereas deformation spreads over a much broader region to the east [e.g., *Buforn et al.*, 1988; *Jiménez-Munt et al.*, 2001; *Zitellini et al.*, 2009]. Deep basins characterize the eastern region of this zone, with bathymetries exceeding −5000 m (Tagus Abyssal Plain, Horseshoe Abyssal Plain, and Seine Abyssal Plain) and separated by high ridges with bathymetries of −100 m (Gorringe Bank and Coral Patch Seamount) (Figure 1). Euler poles derived from paleomagnetic field measurements yield a convergence rate between the African and European plates of ~3.9 mm/yr in an ESE-WNW direction [*Argus et al.*, 1989].

[10] Plate kinematic reconstructions of the Atlantic-Mediterranean region [e.g., *Roest and Srivastava*, 1991; *Rosenbaum et al.*, 2002; *Schettino and Scotese*, 2002; *Stampfli and Borel*, 2002] show that the breakup of the northern segment of the central Atlantic occurred during the Late Jurassic at about 160–150 Ma (Oxfordian-Tithonian times), after a ~20 Ma long period during which Africa drifted SE relative to Iberia. At this stage, the continental crusts of Iberia and Newfoundland were still welded, and the central Atlantic was connected to the Alpine-Tethys Ocean through a narrow corridor, which opened at the end of the Jurassic [e.g., *Schettino and Scotese*, 2002; *Stampfli and Borel*, 2002].

[11] The opening of the North Atlantic started between the upper Berriasian times at ~143 Ma [*Schettino and Scotese*, 2002] and the Valanginian times at ~139 Ma in the Early Cretaceous [*Stampfli and Borel*, 2002]. The northward propagation of the North Atlantic opening reached the northern margin of Iberia in early Albian times at ~110 Ma [*Schettino and Scotese*, 2002]. These ages agree with absolute ages determined on peridotite ridges aligned along the western Iberian Margin during Ocean Drilling Program (ODP). The age of the gabbros in the Gorringe Bank is 143 Ma [*Féraud et al.*, 1996], whereas that at the northern ODP sites 897 and 899 is 136 Ma (leg 149 [*Sawyer et al.*, 1994]). The $^{40}Ar/^{39}Ar$ dating of metagabbros at sites 1068 and 1070 (leg 173 [*Whitmarsh et al.*, 1998]) yielded ages of 122 Ma [*Féraud et al.*, 1996]. After the initiation of the North Atlantic, the motion of Africa and Iberia was similar, and no major changes occurred in the former region of the Gorringe Bank.

[12] After the opening of the Gulf of Biscay and the concomitant counterclockwise rotation of the Iberia and Africa plates as well as their common plate boundary, the onset of north to NNW motion of Africa relative to Europe occurred in the late Campanian at ~72 Ma (C32). From the Late Cretaceous to the late Oligocene, convergence between Africa and Iberia was accommodated mostly by shortening along the northern Iberian Margin. This gave rise to the Pyrenees, which were mostly built up by the end of the Oligocene time, welding Iberia to Eurasia. This represented a quiescent tectonic period at the southern Iberian Margin [e.g., *Vergés et al.*, 2002].

[13] Since the end of the Oligocene, convergence between Africa and Eurasia mostly shifted to the southern Iberian Margin, forming the Betic-Rif System with concomitant consumption of the Late Jurassic Atlantic-Alpine-Tethys transition. The entire Africa-Eurasia plate boundary started to deform, including its westernmost Gorringe Bank basin floored by upper mantle rocks or transitional crust. Tectonic inversion of the previously extended Gorringe Bank region occurred during the Miocene NNW motion of Africa against Eurasia (according to convergence vectors from the work of *DeMets et al.* [1990] and *Argus et al.* [1989]). At present, most of the seismicity is concentrated along the Horseshoe, Marques de Pombal, and Cabo San Vicente thrusts [e.g., *Gràcia et al.*, 2003; *Terrinha et al.*, 2003; *Zitellini et al.*, 2004, 2009] to the SE of the Gorringe Bank.

3. Shallow Structure of the Gorringe Bank and Crustal Shortening

[14] We analyze the shallow structure of the Gorringe Bank in the light of available seismic profiles and geological data with the aim of establishing the main seismic-stratigraphic units and balancing a true depth crustal cross section across it. Therefore, we have revised the Iberian Atlantic Margin- (IAM-) 4 seismic reflection survey already documented by *Tortella et al.* [1997] (Figure 2), which is almost parallel to the seismic reflection line AR92-3 interpreted by *Sartori et al.* [1994]. The sedimentary cover in the IAM-4 profile is well imaged and can be subdivided into several large units that are significant for the structural evolution of the region: precompressive units (pregrowth unit), syncompressive units (growth unit), and late postcompressive

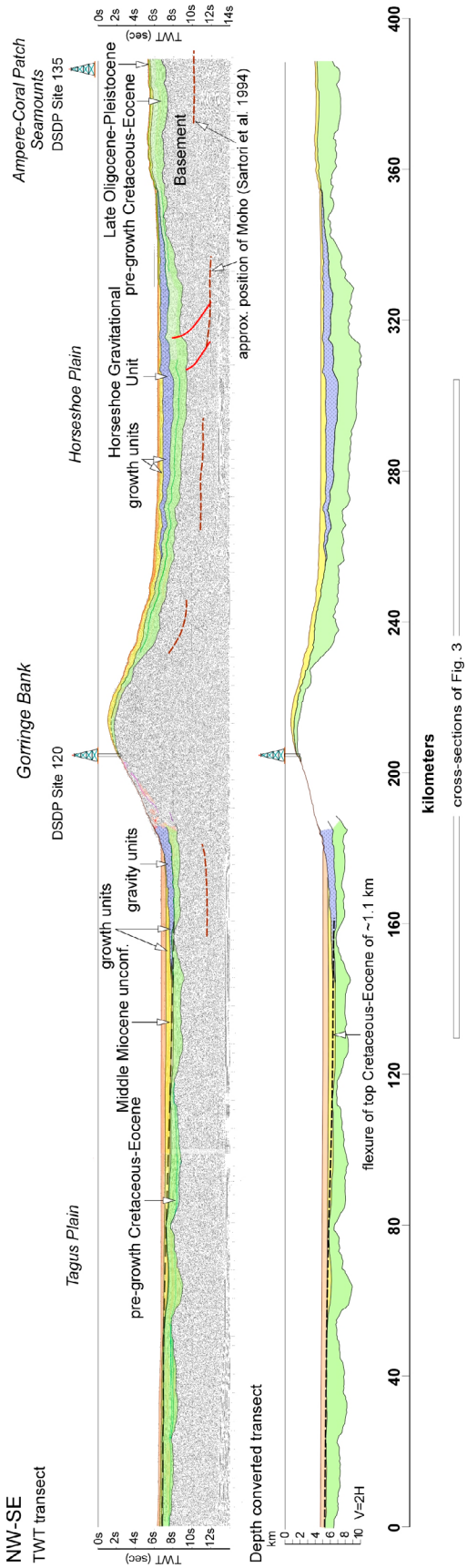

Figure 2. Seismic reflection survey IAM-4 together with line drawing (in two way time and depth converted) for the cover rocks. Its localization is shown in Figures 1 and 4. The Moho depth (red dashed line) is the result of the seismic reflection line AR92-3 [*Sartori et al.*, 1994].

units (postgrowth unit) [*Tortella et al.*, 1997] (Figure 2). The lowermost precompressive units (O1 from the work of *Tortella et al.* [1997]) correspond to Early Cretaceous deposits infilling small basins (10–30 km in width) located between basement structural highs. These basins are better represented in the Tagus Plain on the NW side of the Gorringe Bank. The uppermost part of this precompressive unit is formed by package of more regular thickness encompassing Late Cretaceous, Paleocene, and Eocene deposits (O2 and O3 from the work of *Tortella et al.* [1997]). Pregrowth deposits decrease in thickness toward the top of the Gorringe Bank, where only about one hundred meters of sediments were drilled at DSDP Site 120 [*Ryan et al.*, 1973]. The compressive growth unit (O4 according to *Tortella et al.* [1997]) is interpreted on the basis of its variable thickness across tectonic structures and includes the Horseshoe Gravitational Unit in the Horseshoe Abyssal Plain [e.g., *Iribarren et al.*, 2007], as well as the smaller but significant gravitational units on the lower slope of the northern flank of the Gorringe Bank [e.g., *Sartori et al.*, 1994]. In the Tagus Plain, the growth unit is identified as progressively thickening toward the Gorringe Bank where it onlaps the gravity units. The age of the compressive growth unit is late Oligocene to Miocene [*Lajat et al.*, 1975; *Sartori et al.*, 1994]. The Horseshoe Gravitational Unit, infilling the Horseshoe Plain between the already slightly elevated Ampere-Coral Patch and the Gorringe Bank, has been interpreted as largely derived from the tectonic domain named the Gulf of Cadiz Imbricate Wedge [*Iribarren et al.*, 2007] (Figure 2). The gravitational units located in the forelimb of the Gorringe Bank are thick but of limited area and correspond to the erosion and gravitational collapse of this steeper flank of the ridge. If we assume that the deposition of these gravity units is related to active tectonics, the interdigitation of these units with the lower part of the growth deposits in the Tagus Plain as well as the onlap relation of overlying units might indicate the timing of growth for the Gorringe Bank. Postgrowth deposits correspond to a thin, continuous unit made up of Pliocene and Quaternary pelagic sediments that smoothly draped the bathymetry of the Gorringe Bank (O5 of *Tortella et al.* [1997]).

[15] The IAM-4 seismic line shows two important tectonic features: the folding of pregrowth strata in the SE flank of the Gorringe Bank along the Horseshoe Plain and the progressive down flexure of the top of the pregrowth strata in the Tagus Plain. The structures in the Horseshoe Plain are assumed to be related to NW directed thrusts at depth with a potential strike-slip component, as described by *Rosas et al.* [2009] and *Zitellini et al.* [2009]. To calculate the exact geometry of the hanging wall as well the accurate flexure observed in the Tagus Plain along the footwall of the Gorringe Bank, we converted the two way time (TWT) shallow crustal part (seawater and sedimentary cover) of seismic line IAM-4 to depth using the 2DMove software from Midland Valley. We used velocities of 1500 m/s for seawater, 2250 m/s for the postgrowth unit, 2450 m/s for the growth unit, and 3000 m/s for the pregrowth unit, in fairly good agreement with results proposed by *Gónzalez et al.* [1998]. Once converted, the flexure of the top of the Cretaceous-Eocene pregrowth strata flex down about 1.1 km near the Gorringe Bank with a wavelength of near 100 km (Figure 2). The upper part of the pregrowth strata in the Horseshoe Plain shows near-constant thickness across the basin, and we assume that their top was subhorizontal during deposition. This unit, however, is clearly folded on top of the Gorringe Bank, defining the hanging wall anticline geometry (Figures 2 and 3). If we assume that the Gorringe Bank anticline is related to a thrust and that material in the hanging wall moved parallel to this thrust, then the geometry of the hanging wall anticline might constrain the geometry of the thrust at depth, which is not imaged in any of the seismic lines crossing the Gorringe Bank.

[16] To establish the potential geometry of the thrust fault, we restore the top of the pregrowth strata to horizontal. This surface is reconstructed using the preserved top along the Horseshoe Plain as well as along the southeastern flank and crustal domain of the Gorringe Bank. On the northwestern flank, this surface continues along the present slope of the Gorringe Bank, which constitutes the minimum position of the top of the pregrowth strata unit since it is not preserved there (serpentinized peridotites cropping out; Figure 3). This subhorizontal unfolded position of the pregrowth strata along the forelimb of the anticline will provide a minimum amount of shortening. The top of the pregrowth unit shows a present rounded geometry that can be produced only above a flat-ramp-flat thrust fault geometry, as observed in Figure 3. The reconstructed thrust geometry is subparallel to the top of the pregrowth strata beneath the Horseshoe Plain and the southeastern flank of the Gorringe Bank, whereas the thrust flattens underneath its northwestern flank. The frontal tip of the thrust fault has been located at the base of the slope corresponding to the northwestern flank of the Gorringe Bank, constraining the depth at which the thrust fault is located beneath the Horseshoe Plain (Figure 3).

[17] Considering these geometric constraints, we see that the present shape of the Gorringe Bank formed after a minimum of ~15 km of shortening above the crustal thrust, which must be located about 14 km below the top of the pregrowth unit in the Horseshoe Plain and therefore beneath the Moho imaged by *Sartori et al.* [1994]. The flattening of the thrust fault in the upper mantle below the Moho is needed to create such a large structural relief and might be compared to subcrustal thrusting in other oceanic regions such as Western Africa [*Briggs et al.*, 2009] and in the Indian Ocean [*Delescluse and Chamot-Rooke*, 2008]. If we consider the northwestern gravity deposit to be the result of erosion of the frontal limb of the Gorringe Bank, then we must add ~5 km to the shortening (based on calculation of the area), taking the total shortening for the Gorringe Bank to ~20 km. Our calculated shortening of ~20 km disagrees with the 50 km deduced by *Hayward et al.* [1999]. *Sartori et al.* [1994] proposed shortening of about 10% equally distributed along a 200 km wide region, which results in a much smaller amount than our proposed value for this specific structure, which was ~100 km wide before thrusting (see the restored cross section in Figure 3). Nevertheless, our shortening calculation yields a value similar to that proposed by *Galindo-Zaldívar et al.* [2003].

[18] According to results from DSDP Site 120, at which shallow water deposits corresponding to about the early

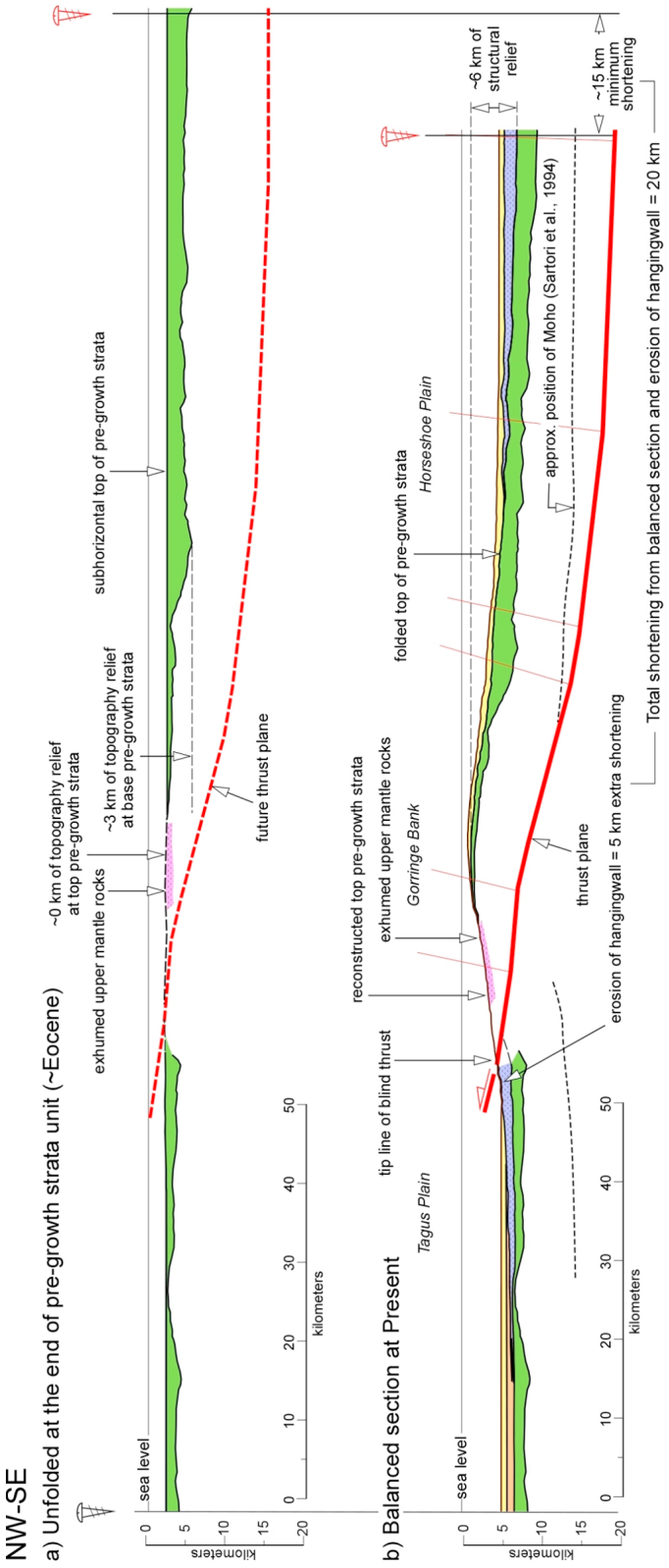

Figure 3. Balanced and unfolded cross sections across the Gorringe Bank based on the IAM-4 seismic line depth conversion (Figure 2). Balanced cross section shows that the potential geometry of the thrust fold at depth matches the geometry of the folded top of pregrowth strata.

Miocene were drilled [*Ryan et al.*, 1973], the Gorringe Bank probably started to grow during the early Miocene or even earlier. A large onlap unconformity along the northwestern flank of the Gorringe Bank [*Mauffret et al.*, 1989], dated as mid-Miocene by seismic correlation to DSDP site 398 [*Sibuet and Ryan*, 1979], indicates that at that time most of the present topography was already created. This also agrees with the confined deposition of the middle-late Miocene Horseshoe Gravitational Unit to the southeast, indicating partial uplift of the Gorringe Bank during its deposition [*Iribarren et al.*, 2007]. However, the smooth folding of the Horseshoe Gravitational Unit in the backlimb of the Gorringe Bank also indicates that some shortening has occurred since its deposition. Considering a constant rate of shortening of ~4 mm/yr, we would obtain a minimum time interval of ~5 Ma for the entire Gorringe Bank to grow (almost entirely within the early Miocene). This implies that the total convergence rate is entirely concentrated at the Gorringe Bank. However, if we consider that only half (1.9 mm/yr) of the total convergence was accommodated in the Gorringe Bank [*Jiménez-Munt and Negredo*, 2003), then the growth would span ~10.5Ma (possibly starting within the late Oligocene or lasting until the middle Miocene). At present, despite the occurrence of some earthquakes beneath the Gorringe Bank, the main zone of active deformation seems to have migrated to the SE, toward the Horseshoe, San Vicente, and Marques de Pombal crustal thrusts [e.g., *Gràcia et al.*, 2003; *Zitellini et al.*, 2009] (Figure 1).

4. Present-Day Lithospheric Structure

[19] In the previous section, we determined the present tectonic structure of the Gorringe Bank above a subcrustal thrust fault, and we proposed the precompression disposition of the bank using true depth-converted balanced and restored cross sections. In this section, we aim to constrain the present-day crustal and lithospheric structure of the Gorringe Bank, and particularly the significance of the large positive geoid and gravity anomalies, in terms of the composition of the crust and upper mantle and isostatic behavior. For this purpose, we have applied a method based on the integration of regional data including elevation, gravity, geoid, and heat flow together with available seismic data and geological constraints from the previous section. The combined interpretation of these data provides information on the density and temperature distributions at different depth ranges. Seismic data provide valuable information on both the geometry of crustal layers and the depth distribution of *P* wave velocities.

4.1. Numerical Method and Regional Data

[20] The geopotential, lithostatic, and heat transport equations were solved simultaneously using a finite-element code based on *Zeyen and Fernàndez* [1994]. This modeling technique has been applied in different geodynamic settings to determine the crustal and lithospheric structure, including the Pyrenees [*Zeyen and Fernàndez*, 1994], the High-Middle Atlas [*Zeyen et al.*, 2005; *Teixell et al.*, 2005], the SW Iberian Margin [*Fernàndez et al.*, 2004b], the mid-Norwegian Margin [*Fernàndez et al.*, 2004a], and the Tibetan Plateau [*Jiménez-Munt et al.*, 2008]. A detailed explanation of the methodology can be found in these previous works.

[21] An initial crustal model is constructed by compiling available seismic data and other geological constraints. The calculated elevation, Bouguer anomaly, geoid height variation, and surface heat flow are compared with the measured values. Then the geometries of the different bodies (crustal layers and lithosphere-asthenosphere boundary) are modified until the best fit is obtained. Clearly, the degree of freedom in modifying the geometry of the crustal layers depends on the availability and quality of geological and seismic data.

[22] Owing to the high topography of the Gorringe Bank, characterized by a high amplitude and relatively short wavelength, we account for the rigidity of the lithosphere to calculate lithostatic equilibrium (flexural isostasy). To compute the elevation for a given lithospheric geometry, we first calculate lateral changes in lithostatic pressure at a compensation level based on the lithospheric structure derived from potential fields. Note that relative lateral variations in pressure are independent of the compensation level as long as it is taken within the asthenosphere, which is here assumed to have a constant density. We then calculate the vertical displacement (deflection) w of every column required to compensate for these pressure variations using different values of elastic thickness T_e ranging from 0 (local isostasy) to 35 km (expected value for a ~140 Ma old oceanic lithosphere [*Watts*, 2001]). Under the elastic thin plate approach, the deflection w of the lithosphere in response to vertical lithostatic pressure variations is given as follows [*Watts*, 2001; *Garcia-Castellanos et al.*, 1997]:

$$D\frac{d^4w(x)}{dx^4} + (\rho_a - \rho_w)gw(x) = q(x) - \overline{q} \qquad D = \frac{ET_e^3}{12(1-\nu^2)},$$

where x is the position along the section, D is the rigidity of the lithosphere, g is the gravitational acceleration (9.8 m/s^2), ρ_a and ρ_w are the densities of the asthenosphere and seawater, respectively (see Table 1), $q - \overline{q}$ is the lithostatic pressure anomaly (relative to the mean pressure along the transect), E is Young's modulus (taken as 7×10^{10} N m), ν is Poisson's coefficient (taken as 0.25), and T_e is the lithospheric elastic thickness (assumed constant along the profile). Because pressure anomalies are calculated from a lithospheric geometry that incorporates the present bathymetry, the calculated deflection should be small in amplitude and induce small changes in bathymetry along the section. This can occur either if the lithospheric section is already under local isostasy (no lateral changes in pressure) or if T_e is high enough to smooth the amplitude of pressure variations. The first is not the case because, as it will be seen, the Gorringe Bank area of the lithospheric section derived from gravity and the geoid is denser than adjacent areas (it produces higher pressure at the compensation level). Therefore, we vary T_e to find the values that reduce the calculated deflection below a certain value.

[23] Regional elevation, geoid, gravity, and heat flow data have been taken primarily from global datasets. Elevation data come from the Geographic Information Network of Alaska (GINA) Global Topo Data (http://www.gina.alaska.edu/), with values in a 30′ grid spacing (Figure 1). Over a distance of

Table 1. Physical Parameters of the Different Bodies Used in the Modeing[a]

Description	ρ (kg/m^3)	K (W/(K·m))	H (μW/m^3)
Sediments	2200–2460	2.0	2.0
Upper crust	2600	2.5	1.0
Lower crust	2900	2.5	0.2
Upper Gorringe (z < 14 km)	2840–3170	2.77	0.02
Deeper Gorringe (z > 14 km)	3180–3290	3.1	0.02
Lithospheric mantle	$3200 \cdot [1–3.5 \times 10^{-5}$ (T-1350°C)]	3.2	0.02

[a]Abbreviations as follows: ρ, density (this density can vary in depth); K, thermal conductivity; H, radiogenic heat production; z, depth. The density of the lithospheric mantle is temperature dependent $T(z)$, $\rho_m = \rho_a[1 - \alpha \cdot (T(z) - T_a)]$, where ρ_a is the density of the asthenosphere (3200 kg/m^3), α is the thermal expansion coefficient (3.5×10^{-5} 1/°C), and T_a is the temperature of the asthenosphere (1350°C). Seawater density ρ_w = 1031 kg/m^3.

100 km, the bathymetry changes from slightly deeper than 5 km in the Tagus Abyssal Plain to near sea level on the highest peaks of the Gorringe Bank and then decreases again to near 5 km in the Horseshoe Abyssal Plain. Geoid height (Figure 4a) is taken from the EGM96 global model [*Lemoine et al.*, 1998]. To avoid the effect of sublithospheric density variations on the geoid, we have removed the geoid signature corresponding to the spherical harmonics developed until degree and order 9. This geoid anomaly also exhibits a large gradient around the Gorringe, with a maximum amplitude exceeding 10 m with respect to the adjacent abyssal plains. The Bouguer gravity anomaly (Figure 4b) is calculated from the global free air anomaly database [*Sandwell and Smith*, 1997] to which a full 3-D topographic correction has been applied following the method outlined by *Fullea et al.* [2008]. The Bouguer gravity anomaly also shows a maximum of ~380 mGal on the Gorringe Bank, and the maximum variation relative to the abyssal plains is ~120 mGal. We have compiled surface heat flow measurements in the area from different authors (colored circles in Figure 4b) [*Verzhbitsky and Zolotarev*, 1989; *Polyak et al.*, 1996; *Fernàndez et al.*, 1998; *Rimi et al.*, 1998; *Grevemeyer et al.*, 2009]. Around the Gorringe Bank there are a few measurements, which vary between 40 and 65 mW/m^2.

4.2. The Lithospheric Cross Section

[24] The modeled 2-D lithospheric profile is 275 km long and follows the IAM-4 seismic reflection survey [*Banda et al.*, 1995; *Tortella et al.*, 1997] from (12°W, 37.4°N) to (10.21°W, 35.5°N) (Figures 1 and 4 for localization and Figure 2 for the seismic line interpretation), which practically overlaps with the seismic reflection line AR92-3 [*Sartori et al.*, 1994]. The profile crosses the Gorringe Bank perpendicularly from the oceanic domain to the NW to the continent-ocean transition lithosphere to the SE [*Rovere et al.*, 2004]. To avoid undesirable edge effects and to ensure a regional fitting of data, we have extended the profile 100 km from each side.

[25] An initial crustal model based mainly on available seismic data was constructed to begin the lithosphere modeling. The geometry of the sediments and crust layers was inferred from seismic profiles IAM-4 and AR92-3 (Figure 2). From line IAM-4, we inferred a sediment thickness between 1.5 and 3.6 km on the NW segment, thinning rapidly toward the pronounced slope of the Gorringe Bank, where it practically disappears. The slope is smoother in the SE of the Gorringe Bank, and a thin sedimentary layer some meters thick also covers the top. This cover becomes progressively thicker southeastward, reaching a thickness of 5.3 km. The AR92-3 seismic line [*Sartori et al.*, 1994] provides information about the Moho depth (Figure 2, dashed line), which according to their velocities varies from 7.2 km in the NW segment to 8.2 km in the SE segment.

[26] Beneath the Gorringe Bank, none of the seismic profiles allow the crustal geometry to be defined. However, the Gorringe diving cruise [*Girardeau et al.*, 1998] showed that the top and the northwestern flank of the Gorringe Bank consist of highly serpentinized peridotites and gabbros in a subhorizontal arrangement, attributed to exhumed upper mantle rocks. Therefore, we have considered a serpentinized peridotite body occupying the entire crest of the Gorringe Bank, where the upper mantle rocks thrust over the southeastern region of the Tagus Plain. Dredged samples indicate that surface rocks consist predominantly of plag-spinel-harzburgites (mantle rocks equilibrated under relatively low pressure-temperature (P-T) conditions) exhibiting ubiquitous (static) serpentinization. The presence of carbonates associated with serpentinites [*Girardeau et al.*, 1998] also evidences a pervasive late low-temperature CO_2 metasomatism [*O'Hanley*, 1996] of these rocks. Although it is difficult to assign specific degrees of serpentinization, the above observations indicate high degrees of alteration close to the surface, with serpentinite and carbonates replacing $\geq$ 60% of the original peridotite. This is undoubtedly associated with a major modification of the bulk rock properties, particularly density and thermal conductivity. Another factor that may have modified the properties of the peridotitic rocks is the extraction of melt during the exhumation of the unit [e.g., *Afonso et al.*, 2007]. However, the volume of volcanic material is modest [*Girardeau et al.*, 1998], suggesting low degrees of partial melting during the extensional regime. This in turn indicates that compositional buoyancy due to partial melting of the peridotites can be omitted.

[27] To calculate the depth-density variation of peridotites, we assume that density varies linearly with the serpentinization fraction. Under normal P-T conditions, plagioclase-spinel peridotites have densities of ~3330 kg/m^3 [e.g., *Lee*, 2003], whereas under the same conditions, the density of a 100% serpentinized peridotite is ~2650 kg/m^3 [*O'Hanley*, 1996]. With these two end-member values, we can com-

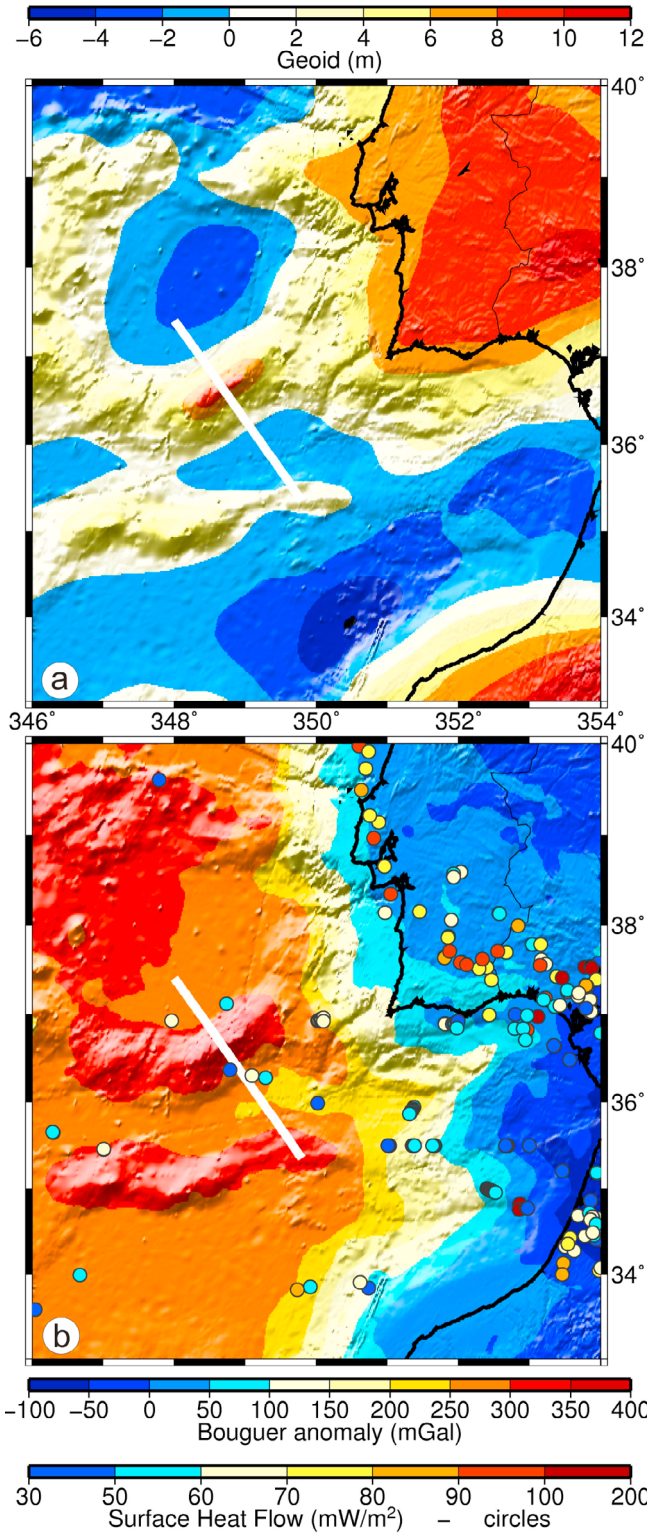

Figure 4. (a) Geoid high and (b) Bouguer gravity anomaly data and measured surface heat flow in circles. Shading indicates elevation data, and bold white line indicates the position of the profile.

pute the density of serpentinized peridotites for any fraction of serpentinization. It is not well known how serpentinization fraction changes with depth; however, there is evidence that vigorous fluid circulation can occur down to 20–25 km in depth in extensional oceanic environments [*Ranero et al.*, 2003]. Additionally, geochemical studies in ophiolites indicate that the maximum depth of serpentinization can reach depths of ~40 km [*Li and Lee*, 2006]. Therefore, we have considered that serpentinization varies from 70% (~2840 kg/m^3) at the surface to 20% (~3170 kg/m^3) at 14 km depth and to 0% (~3280 kg/m^3) at 40 km depth (Figure 5) [*Delescluse and Chamot-Rooke*, 2008]. At this depth (40 km), no compositional density contrast with the surrounding lithospheric mantle exists (Figure 5 and Table 1). The thermal conductivity (K) of serpentinites is significantly smaller than that of fresh peridotites under similar P-T conditions. To account for this effect in our models, we proceed as follows: (1) the thermal conductivity of serpentinites is calculated as a function of P and T following the parameterization proposed by *Seipold and Schilling* [2003]; (2) an average K value is estimated for the serpentinites on each of the segments characterized by 70%–20% and 20%–0% serpentinization, respectively (see Figure 5); and (3) the final thermal conductivity of the partially serpentinized mantle is

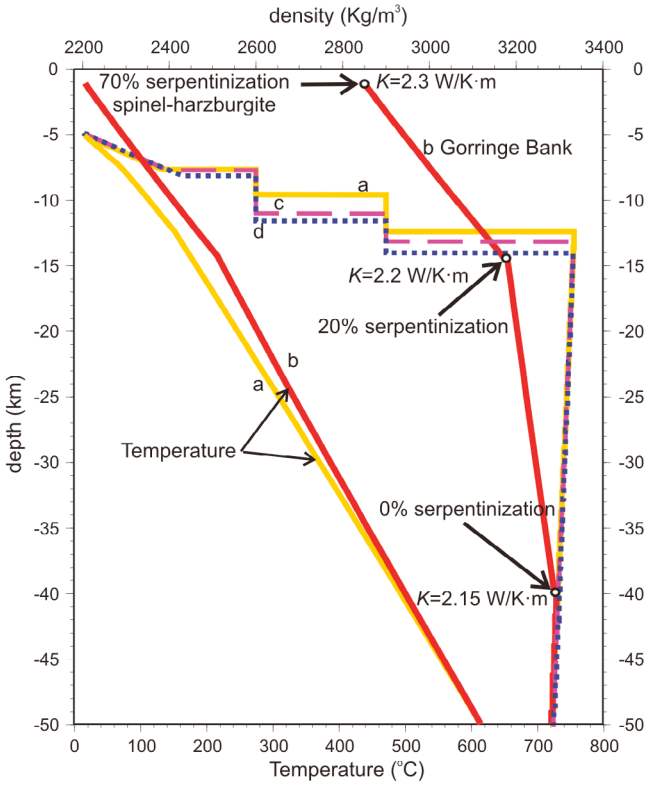

Figure 5. Density and temperature depth profiles at four positions identified in Figure 6d: Tagus Abyssal Plain (profile a), Gorringe Bank (profile b), and Horseshoe Abyssal Plain (profiles c and d). Values of K are conductivities of pure serpentinite at different pressures and temperatures.

then computed as the weighted average of the values for pure serpentinites (K_{serp}) and pure peridotites (K_{perid}) as $K = K_{serp}X_{serp} + K_{perid}X_{perid}$, where X_{serp} and X_{perid} are the volume fractions of serpentinite and peridotite, respectively. The apparently rough approximation described in (2) is justified given the small ($\leq$ 4%) difference in K values within each segment (Figure 5). Table 1 summarizes the values assigned to the physical properties of each body considered in the modeled section.

[28] Figure 6 shows the observed and calculated values of surface heat flow (Figure 6a), Bouguer anomaly (Figure 6b), geoid (Figure 6c), and elevation (Figure 6d) for the lithospheric structure (Figure 6e) that best fits all these observables. The data are represented by dots with dispersion bars, corresponding to the standard deviation within a range of 25 km to each side of the profile, and the lines denote the calculated values from the lithospheric geometry in Figure 6d. The geoid and gravity are fitted within the dispersion bars, whereas the fitting in elevation depends largely on the considered elastic thickness. The calculated surface heat flow is between 45 and 50 mW/m^2 and agrees with typical values obtained for oceanic lithosphere and with six measurements located along the profile (between 40 and 65 mW/m^2; Figures 4b and 6a). The crustal geometry on both sides of the Gorringe Bank is constrained by seismic data. The geometry of the serpentinized peridotite ridge has been obtained on the basis of geological and tectonic considerations and after several attempts to obtain the best fitting with the observables. The resulting body extends down to 40 km depth (with a variable degree of serpentinization) and has a width of 50 km near the surface, narrowing to 30 km at depth. The lithosphere-asthenosphere boundary lies at a depth of 110 km in the NW oceanic domain, dipping progressively to the SE transitional domain down to 120–130 km. A discussion of the significance of the model results is presented in the following section.

5. Discussion

[29] Previous models for the formation of the Gorringe Bank succeeded in explaining subsets of the geological and geophysical observables but failed to give a complete and consistent view of its origin, evolution, and present-day structure. Difficulties arise in reconciling the various crustal/lithospheric structures proposed on the basis of regional observables (geoid, gravity, elevation, and heat flow) with geological constraints on the large-scale tectonic evolution. In particular, the lack of reliable restored cross sections made the proposed models that imply crustal duplication speculative. Other models failed to provide a satisfactory explanation for the presence of a massive peridotite ridge. Furthermore, regional isostasy has often been invoked to account for the topography of the Gorringe Bank, yet the flexural calculations lacked constraints in the adopted load distribution or the resulting vertical motions. With the goal of proposing a model that covers these gaps, we discuss our contribution in the framework of that background, dealing first with the present-day structure and then with the evolution of the Gorringe Bank.

5.1. Present Structure of the Gorringe Bank

[30] One of the first lithospheric models combining different geophysical datasets is from the work of *Souriau* [1984], who analyzed the deep structure of the Gorringe Bank on the basis of geoid, gravity, and bathymetry data and proposed two alternative possibilities: (1) the region is not under local isostasy and corresponds to a nascent subduction zone leading to the superposition of two oceanic crustal layers above the Gorringe Bank and (2) the region is in local isostatic equilibrium, but a low-density root extending to 60 km depth is necessary to fit the geoid and gravity data. According to Souriau, both models encounter serious difficulties regarding compatibility with geological and seismological observations. *Hayward et al.* [1999] presented a crustal model based on seismic reflection and gravity data combined with a flexural analysis. These authors explained the Gorringe Bank structure as the result of ~50 km of thrusting of African oceanic crust upon the Eurasian plate, which behaves as a loaded broken plate with an equivalent elastic thickness of 35 km. Finally, *Galindo-Zaldívar et al.* [2003], using gravity and magnetic data, proposed a model involving 20–30 km of NW verging thrusting of oceanic crust and a nearly flat Moho. Nevertheless, neither the model proposed by *Hayward et al.* [1999] nor that proposed by *Galindo-Zaldívar et al.* [2003] provide a geological explanation for the proposed duplication of the oceanic crust beneath the Gorringe Bank.

[31] Our model incorporates the flexural support of topography with a T_e of 30 km, similar to *Hayward et al.* [1999], and 20 km of NW verging thrusting, similar to *Galindo-Zaldívar et al.* [2003]. However, whereas previous models consider a duplication of the oceanic crust made up of gabbros with some serpentinized peridotites and alkali basalts [*Souriau*, 1984; *Hayward et al.*, 1999; *Galindo-Zaldívar et al.*, 2003] we consider, according to petrological and geological data [*Girardeau et al.*, 1998; *Schärer et al.*, 2000], that the Gorringe Ridge is an upper mantle unit composed mainly of serpentinized peridotites and gabbros that shows no clear genetic association with crustal material. These rocks record a complex tectonic history, as evidenced by their multiple superimposed tectonic fabrics [*Girardeau et al.*, 1998]. We have shown that the lithospheric structure implied by this model is compatible with the measured potential fields and with the balanced and restored cross section along the IAM-4 seismic reflection profile.

[32] The observed maxima in the Bouguer and geoid anomalies at the Gorringe Bank are consistent with the presence of an exhumed piece of lithospheric mantle with high serpentinization at shallow depths, resulting in densities between 2840 and 3170 kg/m^3 from the surface to 14 km depth (Figure 5) and reaching lithospheric mantle densities at a depth of 40 km. These densities correspond to peridotites with ~70% serpentinization near the surface, ~20% at 14 km, and 0% at 40 km depth. Considering a model where the serpentinization in the Gorringe Bank vanishes at 25 km depth results in a modeled Bouguer anomaly and geoid height that exceed the measured values by 10 mGal and 3 m, respectively. If serpentinization is confined to the upper 14 km, the misfits increase to 65 mGal and 8 m for

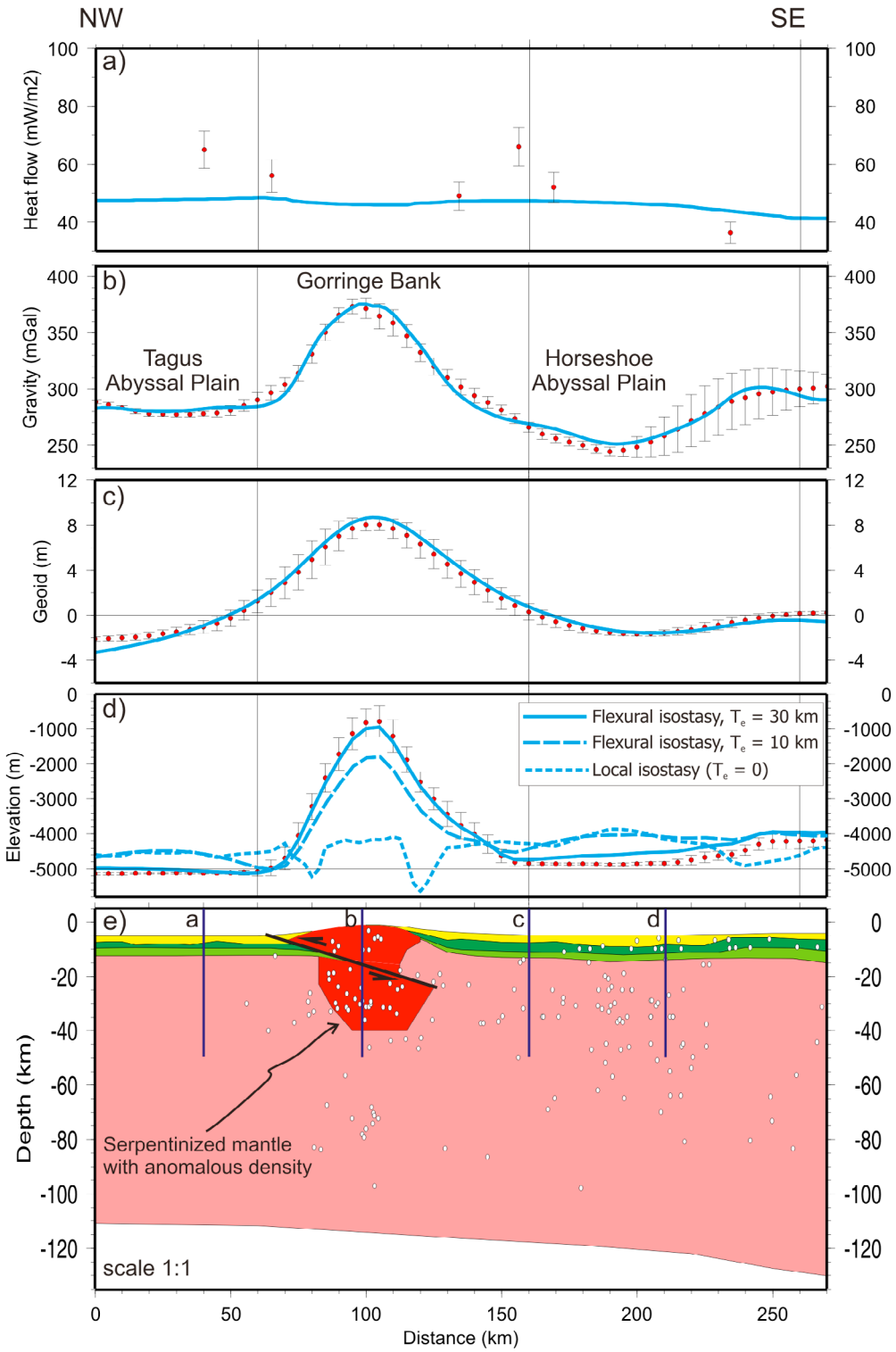

Figure 6. Model results (blue lines) and measured data with the standard deviation of 25 km to each side of the profile (red dots and vertical bars): (a) surface heat flow, (b) Bouguer anomaly, (c) geoid, (d) elevation, and (e) lithosphere structure. Vertical blue lines are the positions of the density profiles shown in Figure 5. White dots are earthquake hypocenters projected onto the model section from a 100 km wide strip (data taken from Instituto Geográfico Nacional, Spain, http://www.ign.es). Line patterns in Figure 6c indicate different elastic thickness values used to isostatically compensate for the lithospheric structure shown in Figure 6d.

the Bouguer anomaly and geoid height, respectively. Both gravity anomaly and geoid height are sensitive mainly to the average density such that varying the depth distribution of serpentinization has no major effects provided that the average density is not changed.

[33] The presence of serpentinites beneath the Gorringe Bank is likely to reduce friction along pre-existing fault planes [e.g., *Escartín et al.*, 2001], thus favoring the localization and persistence of thrusting during the Miocene shortening. The results suggest that the bulk of the Gorringe Bank topography cannot be sustained by a weak lithosphere of $T_e \approx 0$ (local isostasy) or $T_e < 15$ km (Figure 6c). In contrast, T_e values larger than 25–30 km satisfactorily explain the topographic profile because pressure anomalies, ranging from 60 MPa under the Gorringe Bank to −20 MPa in the abyssal plains, are compensated for and cancelled out over long distances. Such T_e values are in agreement with our suggestion that deep and pervasive serpentinization of the mantle beneath the Gorringe Bank occurred simultaneously with the generation of extensional faults and mantle exhumation during the Late Jurassic and Early Cretaceous periods (~140 Ma). After this main extensional event, the thermal structure of the region followed a normal cooling history. The overall calculated lithospheric temperature distribution follows the geotherm predicted by the cooling plate model [*Parsons and Sclater*, 1977], whereas the required lithospheric rigidity is consistent with the elastic thicknesses obtained in other oceanic areas of similar age to the Gorringe Bank ($T_e = 35 \pm 15$ km for a 140 Ma old plate [*Watts*, 2001]).

[34] Lateral T_e variations may be expected due to serpentinization beneath the Gorringe Bank and to lateral temperature changes along the transect (less than 40° at 15 km depth; Figure 5). However, owing to the short wavelength of the serpentinized body, our method does not allow discrimination of such T_e changes.

[35] A priori, an alternative to explain the high topography of the Gorringe Bank by local isostasy would be to consider a deeper low-density root with a linear decrease in the density contrast relative to the contiguous lithospheric mantle. The best results are obtained for a density contrast changing from 160 kg/m^3 at 14 km depth (20% of serpentinization) to 0 kg/m^3 (0% of serpentinization) at 100 km. However, *Souriau* [1984] already noted that serpentinite is not stable at temperatures above 500–700°C [*Ulmer and Trommsdorff*, 1995], and therefore it is unlikely that serpentinization affects peridotites at depths below 40–60 km [e.g., *Delescluse and Chamot-Rooke*, 2008] (see also Figure 5).

5.2. Evolution of the Gorringe Bank

[36] The combination of the present-day lithospheric structure and crustal restoration with results from previous studies allows reconstruction of the large-scale tectonic evolution for the Gorringe Bank region from Late Jurassic to Recent. This evolution is presented in four sequential schematic maps and cross sections (Figure 7) summarizing the evolution of the area between the central and North Atlantic oceanic realms that was connected to the Alpine-Tethys Ocean from the Late Jurassic to mid-Tertiary and subsequently connected to the Western Mediterranean Sea. In these maps we use as a reference the present coastlines of Iberia and northern Africa, which are moved according to the plate displacement vectors proposed by *Rosenbaum et al.* [2002]. The transtensive geometry of the Africa-Iberia plate boundary has been constructed in agreement with the plate reconstructions by *Schettino and Scotese* [2002] and *Stampfli and Borel* [2002].

[37] The first stage (Late Jurassic) corresponds to the opening of both the northern segment of the central Atlantic Ocean and its connection with the Alpine-Tethys Ocean to the east (Figure 7a). This transtensional phase separated Iberia-Newfoundland from Africa after a period of about 20 Ma of strike-slip motion between these two plates that separated the continental and oceanic domains. *Rovere et al.* [2004] proposed that the paleo Iberia-Africa plate boundary (PIAB) presently extends south of the Gorringe Bank, separating the oceanic domain of the African plate from the continental-transitional domain of the Iberian plate. However, according to these authors, the extent of the African oceanic domain as well as the continuation of the PIAB east of the Coral Patch Seamount is uncertain. On the basis of plate reconstruction models, several authors have proposed an irregular geometry for the plate boundary in this area, implying a segmentation of the African and Iberian margins [e.g., *Klitgord and Schouten*, 1986; *Srivastava et al.*, 1990; *Roest and Srivastava*, 1991]. Bearing in mind the uncertainties in all these models and the available data, we speculate that the differential transtensional motion between Africa and Iberia was accommodated by transform faults

Figure 7. Four schematic geological maps defining the evolution of the Atlantic-Alpine Tethys transition and the corresponding cross sections perpendicular to the Gorringe Bank (red line in maps). (a) Late Jurassic extension of continental crust with mantle exposed at the transition between central Atlantic and Alpine-Tethys oceans after ~20 Ma of eastward African drifting. In the cross section, we add the position of the future North Atlantic ridge at about 140 Ma along the exhumed mantle and continental crust boundary. (b) Early Cretaceous serpentinization and gabbroic intrusions affected the exhumed upper mantle rocks during the initiation of the northern propagation of the Atlantic Ocean. (c) At the end of the Late Cretaceous, serpentinized peridotites of the proto-Gorringe Bank separated transitional Africa crust to the SE from Atlantic oceanic crust to the NW at the initiation of Africa-Iberia convergence. (d) Miocene shortening across the Gorringe Bank produced NW directed thrusting of part of the serpentinized peridotites on top of the oceanic and sedimentary cover of the Tagus Plain. Bold dotted line in maps shows the position of the ocean-continent transition zone according to *Rovere et al.* [2004]. Present-day coastlines are merely used to indicate the relative plate movements as derived from *Rosenbaum et al.* [2002]. The width of both the central and northern Atlantic oceanic domains is only illustrative.

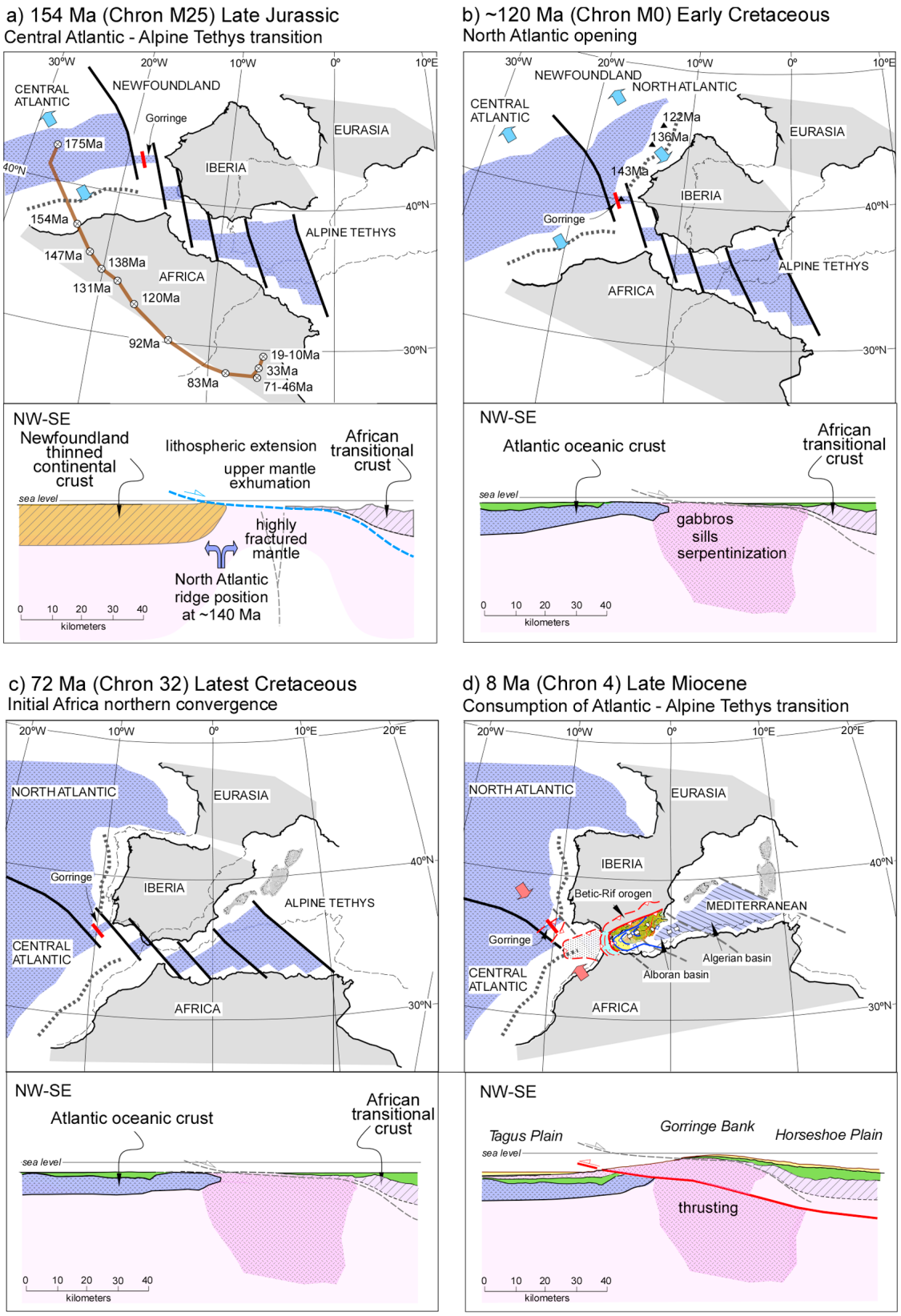
a) 154 Ma (Chron M25) Late Jurassic
Central Atlantic - Alpine Tethys transition
30°W
20°W
10°W
0°
10°E
CENTRAL ATLANTIC
NEWFOUNDLAND
Gorringe
EURASIA
175Ma
40°N
IBERIA
40°N
154Ma
ALPINE TETHYS
147Ma
138Ma
AFRICA
131Ma
120Ma
92Ma
30°N
19-10Ma
33Ma
83Ma
71-46Ma
NW-SE
Newfoundland thinned continental crust
lithospheric extension
upper mantle exhumation
African transitional crust
sea level
highly fractured mantle
North Atlantic ridge position at ~140 Ma
0 10 20 30 40
kilometers
b) ~120 Ma (Chron M0) Early Cretaceous
North Atlantic opening
30°W
20°W
10°W
0°
10°E
NEWFOUNDLAND
NORTH ATLANTIC
CENTRAL ATLANTIC
122Ma
136Ma
EURASIA
143Ma
IBERIA
40°N
Gorringe
ALPINE TETHYS
AFRICA
30°N
NW-SE
Atlantic oceanic crust
African transitional crust
sea level
gabbros
sills
serpentinization
0 10 20 30 40
kilometers
c) 72 Ma (Chron 32) Latest Cretaceous
Initial Africa northern convergence
20°W
10°W
0°
10°E
20°E
NORTH ATLANTIC
EURASIA
40°N
Gorringe
IBERIA
ALPINE TETHYS
CENTRAL ATLANTIC
AFRICA
30°N
NW-SE
Atlantic oceanic crust
African transitional crust
sea level
0 10 20 30 40
kilometers
d) 8 Ma (Chron 4) Late Miocene
Consumption of Atlantic - Alpine Tethys transition
20°W
10°W
0°
10°E
20°E
NORTH ATLANTIC
EURASIA
IBERIA
40°N
Betic-Rif orogen
MEDITERRANEAN
Gorringe
Algerian basin
CENTRAL ATLANTIC
Alboran basin
AFRICA
30°N
NW-SE
Tagus Plain
Gorringe Bank
Horseshoe Plain
sea level
thrusting
0 10 20 30 40
kilometers

Figure 7

and by small extensional basins with a NNW-SSE direction of extension, arranged along the central Atlantic-Alpine-Tethys connection [see also *Le Gall et al.*, 1997; *Olivet*, 1996; *Dercourt et al.*, 1993]. The westernmost of these basins corresponds to the original location of the present Gorringe Bank, which would be limited by two transform faults, the southern one corresponding to the PIAB proposed by *Rovere et al.* [2004] (Figure 7a). In our reconstruction, we assume the formation of a low-angle extensional fault dipping to the SE to create crustal thinning. Nevertheless, a dipping angle to the NW would also be possible. Regardless of the polarity of the low-angle fault, the very slow continental rifting produced the exhumation of peridotitic upper mantle rocks, similar to that in some places from the West Iberian Margin (see IAM-9 profile results [*Pérez-Gussinyé et al.*, 2001]). The exhumed upper mantle blocks were highly fractured and subsequently intruded by gabbros, possibly in connection with mantle thinning. Initial serpentinization, however, would have started at depth before the final exhumation of the mantle rocks.

[38] The second stage of evolution corresponds to the Early Cretaceous at about 120 Ma when continental breakup between Iberia and Newfoundland occurred with the opening of the North Atlantic (Figure 7b). Magnetic anomalies show that the opening of the North Atlantic began along the northwestern side of the proto-Gorringe Bank, producing metasomatism and further serpentinization in the exhumed gabbros and upper mantle rocks. Although not represented in our simplified models in Figure 7b, a normal fault system similar to the one observed along the western Iberian Margin [e.g., *Pérez-Gussinyé et al.*, 2001] could affect the northwestern side of the proto-Gorringe Bank. This scenario produces an asymmetric lithospheric structure on both sides of the serpentinized peridotite ridge (future Gorringe Bank) as inferred from magnetic and seismic data [e.g., *Rovere et al.*, 2004]. To the SE of the peridotite ridge, the basement is formed by African transitional crust, whereas to the NW the basement corresponds to the North Atlantic oceanic domain. The width of this exhumed peridotite strip is uncertain and could extend some km to the NW and SE from the present Gorringe Bank as proposed by *Sallarès et al.* [2010] from preliminary interpretations of a recent wide-angle seismic survey. It is important to notice that the transitional character of the SE crustal domain of the Gorringe Bank is in agreement with the interpretation by *Rovere et al.* [2004], although the plate to which it belongs differs.

[39] The third stage of evolution (Late Cretaceous at about 72 Ma) shows the reconstructed geometry of the proto-Gorringe Bank just before the onset of convergence between the African and Iberian plates (Figure 7c). The small basins of the central Atlantic-Alpine-Tethys connection were covered by sediments, as observed today [e.g., *Tortella et al.*, 1997; *Hayward et al.*, 1999]. These sediments covering the proto-Gorringe Bank region thin dramatically from about 3000 m to the SE to a few tens of meters on the crest of the structure because of the structural relief developed during extension and exhumation in previous stages (see Figure 3). It is worth noting that this relief does not affect our shortening calculations since in the cross section restoration we used the top of the pregrowth unit (Late Cretaceous) as a near-horizontal surface (Figures 3 and 7c). During this stage, the proto-Gorringe Bank was located very close to the plate boundary between Iberia and Africa (Figure 7c).

[40] The fourth and last stage presented in this evolution corresponds to the late Miocene (at about 8 Ma), representing most of the major compressive event affecting the Gorringe Bank and being responsible for the total or partial consumption of the small basins that formed the Iberian-African segmented margin (Figure 7d). Regional thrusting along the uppermost lithospheric mantle hit the serpentinized body at around 14 km depth and carried the hanging wall (serpentinized body and African transitional crust) to the NW on top of the Atlantic oceanic crust that characterizes the Tagus Plain. This crustal-scale thrusting produced about 100 km wide and 1.1 km flexural down bending of the Tagus Plain as well as about 20 km of shortening. The flat-ramp-flat geometry of the thrust is determined from the antiformal geometry exhibited by the top of the pregrowth unit. The thrust flattens at depth in the uppermost mantle and may act as a subcrustal detachment level for the currently active Horseshoe, Marques de Pombal, and Cabo San Vicente thrusts to the SE [*Gràcia et al.*, 2003; *Zitellini et al.*, 2009]. The observed geometry of both pregrowth and growth strata, clearly folded in the SE flank of the Gorringe Bank, indicates a post-Eocene folding stage above a blind thrust (Figure 3b). This folding is incompatible with the preserved structural high of the Gorringe Bank since the Late Jurassic and calls into question a possible transverse ridge origin in the sense of *Bonatti* [1978] as invoked by *Conti et al.* [2004]. During this stage, the former African-Iberian plate boundary from the Gorringe Bank to the western Mediterranean is completely deformed by a series of thrusts and stacked units forming a wide and diffuse plate boundary, as has been widely proposed by many authors using seismicity [e.g., *Grimison and Chen*, 1986; *Buforn et al.*, 1988], multichannel seismic [e.g., *Sartori et al.*, 1994], and numerical approaches [e.g., *Jiménez-Munt et al.*, 2001]. Recently, *Zitellini et al.* [2009], on the basis of a swath bathymetry compilation, described a set of linear and subparallel dextral strike-slip faults connecting the Gloria Fault to the Rif-Tell Fault Zone, which is interpreted as a precursor to the formation of a new transcurrent plate boundary between Eurasia and Africa. This strike-slip fault system would be only ~1.8 Ma old [*Rosas et al.*, 2009].

6. Concluding Remarks

[41] The analyses presented in this paper allow us to draw the following conclusions.

[42] 1. The model proposed here for the deep structure and evolution of the Gorringe Bank is consistent with gravity, geoid, elevation, geothermal, and petrological data and with structural geology derived from seismic data.

[43] 2. The high positive gravity and geoid anomalies measured along the Gorringe Bank are consistent with a density anomaly resulting from a massive peridotitic ridge with a depth-dependent degree of serpentinization varying from 70% at the surface to 20% at 14 km depth and 0% at

40 km depth, presently folded above a low-angle subcrustal thrust fault.

[44] 3. The ~5000 m topographic relief at the Gorringe Bank is supported mostly by regional isostasy. The lithospheric flexural behavior implies an elastic thickness of at least 30 km, in agreement with the age of the oceanic lithosphere in this region (~140 Ma). Flexural isostasy is also required to account for the large gravity and geoid anomalies.

[45] 4. The present structure of the Gorringe Bank is the product of a large NW directed subcrustal thrust, with a flat-ramp-flat geometry carrying deformed upper mantle rocks and transitional African crust on top of the bended Eurasian oceanic crust in the Tagus Abyssal Plain. Shortening along the thrust fault is at least 20 km, which probably occurred in a relatively short period of time (~5–10.5 Ma) starting within the late Oligocene or early Miocene and ending in the middle Miocene.

[46] 5. We speculate that the transtensional regime prevailing during the Late Jurassic gave rise to the opening of small basins separated by transform faults along the connecting zone between the central Atlantic and the Alpine-Tethys. Slow lithospheric extension along the westernmost of these basins (the proto-Gorringe Bank) exhumed highly fractured upper mantle peridotites that were further serpentinized and intruded by gabbros during the northern propagation of the North Atlantic Ocean during Early Cretaceous times. The subsequent tectonic quiescence resulted in seafloor subsidence and sedimentary deposition until late Oligocene-early Miocene times, when ongoing Africa-Eurasia convergence induced thrusting of the Gorringe peridotite ridge above the oceanic Tagus Abyssal Plain to the NW.

[47] 6. Our model results support the hypothesis of a large lithospheric extensional detachment later reactivated as a thrust to explain the present structure of the Gorringe Bank, rather than that of a transverse ridge with a morphology basically preserved since the Late Jurassic.

[48] **Acknowledgments.** This research was partly financed by Projects TopoAtlas (CGL2006-05493/BTE), TopoMed (CGL2008-03474-E/BTE), ESF-Eurocores 07-TOPOEUROPE-FP006, SISAT (CGL2008-01124-E/BTE), ATIZA (CGL2009-09662-BTE), and the Consolider-Ingenio 2010 Topo-Iberia (CSD2006-00041). We thank Astrid Mansilla for helping us with the interpretation of the IAM-4 profile. Depth conversion of IAM-4 has been performed using Midland Valley software 2DMove with the help of Eduard Saura. We are indebted to three anonymous reviewers and the Associate Editor who patiently revised and largely improved the former versions of this manuscript. This is contribution 624 from the Australian Research Council National Key Centre for the Geochemical Evolution and Metallogeny of Continents.

References

Afilhado, A., L. Matias, H. Shiobara, A. Hirn, L. Mendes-Victor, and H. Shimamura (2008), From unthinned continent to ocean: The deep structure of the West Iberia passive continental margin at 38°N, *Tectonophysics*, *458*, 9–50.

Afonso, J. C., G. Ranalli, and M. Fernàndez (2007), Density structure and buoyancy of the oceanic lithosphere revisited, *Geophys. Res. Lett.*, *34*, L10302, doi:10.1029/2007GL029515.

Argus, D. F., R. G. Gordon, C. DeMets, and S. Stein (1989), Closure of the Africa-Eurasia-North America plate motion circuit and tectonics of the Gloria fault, *J. Geophys. Res.*, *94*(B5), 5585–5602.

Auzende, J. M., et al. (1984), Intraoceanic tectonism on the Gorringe Bank: Observations by submersible, in *Ophiolites and Oceanic Lithosphere*, edited by I. G. Gass, S. J. Lippard, and A. W. Shelton, *Geol. Soc. Spec. Publ.*, 13, 113–120.

Banda, E., M. Torne, and the IAM Group (1995), Iberian Atlantic Margins Group investigates deep structure of ocean margins, *Eos Trans. AGU*, *76*(3), 25–29.

Bergeron, A., and J. Bonnin (1991), The deep structure of Gorringe Bank (NE Atlantic) and its surrounding area, *Geophys. J. Int.*, *105*, 491–502.

Bonatti, E. (1978), Vertical tectonism in oceanic fracture zones, *Earth Planet. Sci. Lett.*, *37*, 369–379.

Briggs, S. E., R. J. Davies, J. Cartwright, and R. Morgan (2009), Thrusting in oceanic crust during continental drift offshore Niger Delta, equatorial Africa, *Tectonics*, *28*, TC1004, doi:10.1029/2008TC002266.

Buforn, E., A. Udías, and M. A. Colombás (1988), Seismicity, source mechanisms and tectonics of the Azores-Gibraltar plate boundary, *Tectonophysics*, *152*, 89–118.

Conti, M. A., G. de Alteriis, M. C. Marino, G. Pallini, and R. Tonielli (2004), Discovery of Late Jurassic fossils inside modern sediments at Gorringe Bank (eastern Atlantic Ocean) and some geological implications, *Terra Nova*, *16*, 331–337.

Delescluse, M., and N. Chamot-Rooke (2008), Serpentinization pulse in the actively deforming central Indian Basin, *Earth Planet. Sci. Lett.*, *276*, 140–151.

DeMets, C., R. G. Gordon, D. F. Argus, and S. Stein (1990), Current plate motions, *Geophys. J. Int.*, *101*, 425–478.

Dercourt, J., L. E. Ricou, and B. Vrielynck (1993), *Atlas of Tethys Palaeoenvironmental Maps*, Comm. de la Carte Geol. du Mond., Paris.

Escartín, J., G. Hirth, and B. Evans (2001), Strength of slightly serpentinized peridotites: Implications for the tectonics of oceanic lithosphere, *Geology*, *29*, 1023–1026.

Féraud, G., M.-O. Beslier, and G. Cornen (1996), $^{40}Ar/^{39}Ar$ dating of gabbros from the ocean-continent transition of the western Iberia Margin: Preliminary results, *Proc. Ocean Drill. Program Sci. Results*, *149*, 489–495.

Fernàndez, M., I. Marzán, A. Correia, and E. Ramalho (1998), Heat flow, heat production, and lithospheric thermal regime in the Iberian Peninsula, *Tectonophysics*, *291*, 29–53.

Fernàndez, M., M. Torne, D. Garcia-Castellanos, J. Vergés, W. Wheeler, and R. Karpuz (2004a), Deep structure of the Voring Margin: The transition from a continental shield to a young oceanic lithosphere, *Earth Planet. Sci. Lett.*, *221*, 131–144.

Fernàndez, M., I. Marzán, and M. Torne (2004b), Lithospheric transition from the Variscan Iberian Massif to the Jurassic oceanic crust of the central Atlantic, *Tectonophysics*, *386*, 97–115.

Fullea, J., M. Fernández, and H. Zeyen (2008), FA2BOUG—A FORTRAN 90 code to compute Bouguer gravity anomalies from gridded free air anomalies: Application to the Atlantic-Mediterranean transition zone, *Comput. Geosci.*, *34*, 1665–1681, doi:10.1016/j.cageo.2008.02.018.

Galindo-Zaldívar, J., A. Maldonado, and A. A. Schreider (2003), Gorringe Ridge gravity and magnetic anomalies are compatible with thrusting at crustal scale, *Geophys. J. Int.*, *153*, 586–594.

Garcia-Castellanos, D., M. Fernàndez, and M. Torné (1997), Numerical modeling of foreland basin formation: A program relating thrusting, flexure, sediment geometry and lithosphere rheology, *Comput. Geosci.*, *23*(9), 993–1003, doi:10.1016/S0098-3004(97)00057-5.

Girardeau, J., G. Cornen, M.O. Beslier, B. Le Gall, C. Monnier, P. Agrinier, G. Dubuisson, L. Pinheiro, A. Ribeiro, and H. Whitechurch (1998), Extensional tectonics in the Gorringe Bank rocks, eastern Atlantic ocean: Evidence of an oceanic ultra-slow mantellic accreting centre, *Terra Nova*, *10*, 330–336.

González, A., D. Córdoba, R. Vegas, and L. M. Matias (1998), Seismic crustal structure in the southwest of the Iberian Peninsula and the Gulf of Cadiz, *Tectonophysics*, *296*, 317–331.

Gràcia, E., J. J. Dañobeitia, J. Vergés, and PARSIFAL Team (2003), Mapping active faults offshore Portugal (36°N–38°N): Implications for seismic hazard assessment in the SW Iberian Margin, *Geology*, *31*, 83–86.

Grevemeyer, I., N. Kaul, and A. Kopf (2009), Heat flow anomalies in the Gulf of Cadiz and off Cape San Vicente, Portugal, *Mar. Pet. Geol.*, *26*, 795–804.

Grimison, N. L., and W. P. Chen (1986), The Azores-Gibraltar plate boundary: Focal mechanisms, depths of earthquakes, and their tectonic implications, *J. Geophys. Res.*, *91*(B2), 2029–2047.

Hayward, N., A. B. Watts, G. K. Westbrook, and J. S. Collier (1999), A seismic reflection and GLORIA study of compressional deformation in the Gorringe Bank region, eastern North Atlantic, *Geophys. J. Int.*, *138*, 831–850.

Iribarren, L., J. Vergés, F. Camurri, J. Fullea, and M. Fernàndez (2007), The structure of the Atlantic-Mediterranean transition zone from the Alboran Sea to the Horseshoe Abyssal Plain (Iberia-Africa plate boundary), *Mar. Geol.*, *243*, 97–119, doi:110.1016/j.margeo.2007.1005.1011.

Jiménez-Munt, I., and A. Negredo (2003), Neotectonic modelling of the western part of the Africa-Eurasia plate boundary: From the Mid-Atlantic ridge to Algeria, *Earth Planet. Sci. Lett.*, *205*, 257–271.

Jiménez-Munt, I., M. Fernàndez, M. Torné, and P. Bird (2001), The transition from linear to diffuse plate boundary in the Azores-Gibraltar region: Results from a thin-sheet model, *Earth Planet. Sci. Lett.*, *192*, 175–189.

Jiménez-Munt, I., M. Fernàndez, J. Vergés, and J. P. Platt (2008), Lithosphere structure underneath the

Tibetan Plateau inferred from elevation, gravity and geoid anomalies, *Earth Planet. Sci. Lett.*, *267*, 276–289.

Klitgord, K. D., and H. Schouten (1986), Plate kinematics of the central Atlantic, in *The Geology of North America*, vol. M, *The Western North Atlantic Region*, edited by P. R. Vogt and B. E. Tucholke, pp. 351–378, Geol. Soc. of Am., Boulder, Colo.

Lajat, D., B. Biju-Duval, R. Gonnard, J. Letouzey, and E. Winnock (1975), Prolongement dans l'Atlantique de la partie externe de l'Arc bético-rifian, *Bull. Soc. Geol. France*, *17*, 481–485.

Lee, C.-T. (2003), Compositional variation of density and seismic velocities in natural peridotites at STP conditions: Implications for seismic imaging of compositional heterogeneities in the upper mantle, *J. Geophys. Res.*, *108*(B9), 2441, doi:10.1029/2003JB002413.

Le Gall, B., A. Piqué, J.-P. Réhault, M. Specht, and J. Malod (1997), Structure et mise en place d'une ride océanique dans un contexte de limite de plaques convergentes: Le banc de Gorringe (SW Ibérie), *C. R. Acad. Sci., Ser. IIa Sci. Terre Planetes*, *325*, 853–860.

Lemoine, F. G., et al. (1998), The development of the Joint NASA GSFC and NIMA geopotential model EGM96, report, NASA Goddard Space Flight Cent., Greenbelt, Md.

Le Pichon, X., J. Bonnin, and G. Pautot (1970), The Gibraltar end of the Azores-Gibraltar plate boundary: An example of compressive tectonics, paper presented at Upper Mantle Committee Symposium, Flagstaff, Ariz.

Li, Z. A., and C. A. Lee (2006), Geochemical investigation of serpentinized oceanic lithospheric mantle in the Feather River Ophiolite, California: Implications for the recycling rate of water by subduction, *Chem. Geol.*, *235*, 161–185.

Mauffret, A., D. Mougenot, P. R. Miles, and J. A. Malod (1989), Cenozoic deformation and Mesozoic abandoned spreading centre in the Tagus Abyssal Plain (west Portugal): Results of a multichannel seismic survey, *Can. J. Earth Sci.*, *26*, 1101–1123.

O'Hanley, D. S. (1996), *Serpentinites: Records of Tectonic and Petrological History*, *Oxford Monogr. Ser.*, vol. 34, 277 pp., Oxford Univ. Press., Oxford, U. K.

Olivet, J.-L. (1996), Kinematics of the Iberian plate, *Bull. Cent. Rech. Explor. Prod. Elf Aquitaine*, *20*, 131–195.

Parsons, B., and J. G. Sclater (1977), An analysis of the variation of ocean floor bathymetry and heat flow with age, *J. Geophys. Res.*, *82*(5), 803–827.

Pérez-Gussinyé, M., T. J. Reston, and J. P. Morgan (2001), Serpentinisation and magmatism at non-volcanic margins—The effect of the initial lithospheric structure, *Geol. Soc. Spec. Publ.*, *187*, 551–576.

Pinheiro, L. M., R. B. Whitmarsh, and P. R. Miles (1992), The ocean-continent boundary off the western continental margin of Iberia-II: Crustal structure in the Tagus Abyssal Plain, *Geophys. J. Int.*, *109*, 106–124.

Polyak, B. G., et al. (1996) Heat flow in the Alboran Sea, western Mediterranean, *Tectonophysics*, *263*, 191–218.

Purdy, G. M. (1975), The eastern end of the Azores-Gibraltar plate boundary, *R. Astron. Soc. Geophys. J.*, *43*, 973–1000.

Ranero, C. R., J. P. Morgan, K. McIntosh, and C. Reichert (2003), Bending-related faulting and mantle serpentinization at the Middle America Trench, *Nature*, *425*, 367–373.

Rimi, A., A. Chalouan, and L. Bahi (1998), Heat flow in the westernmost part of the Alpine Mediterranean system (the Rif, Morocco), *Tectonophysics*, *285*, 135–146.

Roest, W. R., and S. P. Srivastava (1991), Kinematics of the plate boundaries between Eurasia, Iberia, and Africa in the North Atlantic from the Late Cretaceous to the present, *Geology*, *19*, 613–616.

Rosas, F. M., J. C. Duarte, P. Terrinha, V. Valadares, and L. Matias (2009), Morphotectonic characterization of major bathymetric lineaments in Gulf of Cadiz (Africa-Iberia plate boundary): Insights from analogue modelling experiments, *Mar. Geol.*, *261*, 33–47, doi:10.1016/j.margeo.2008.08.002.

Rosenbaum, G., G. S. Lister, and C. Duboz (2002), Relative motions of Africa, Iberia and Europe during Alpine orogeny, *Tectonophysics*, *359*, 117–129.

Rovere, M., C. R. Ranero, R. Sartori, L. Torelli, and N. Zitellini (2004), Seismic images and magnetic signature of the Late Jurassic to Early Cretaceous Africa-Eurasia plate boundary off SW Iberia, *Geophys. J. Int.*, *158*, 554–568.

Ryan, W. B. F., K. J. Hsü, M. B. Cita, P. Dumitrica, J. Lort, W. Maync, W. D. Nesteroff, G. Pautot, H. Stradner, and F. C. Wezel (1973), Gorringe Bank—Site 120, *Initial Rep. Deep Sea Drill. Proj.*, *13*, 19–41, doi:10.2973/dsdp.proc.2913.2102.1973.

Sallarès, V., S. Martínez-Loriente, A. Gailler, R. Bartolomé, M. A. Gutscher, D. Graindorge, and E. Gràcia (2010), Seismic structure of the main geological provinces off the SW Iberian Margin: First results from the NEAREST-SEIS wide-angle seismic survey, *Geophys. Res. Abstr.*, *12*, EGU2010-4971.

Sandwell, D. T., and W. H. F. Smith (1997), Marine gravity from Geosat and ERS 1 satellite altimetry, *J. Geophys. Res.*, *102*(B5), 10,039–10,054.

Sartori, R., L. Torelli, N. Zitellini, D. Peis, and E. Lodolo (1994), Eastern segment of the Azores-Gibraltar line (central-eastern Atlantic): An oceanic plate boundary with diffuse compressional deformation, *Geology*, *22*, 555–558.

Sawyer, D. S., et al. (1994), *Proceedings of the Ocean Drilling Program*, Initial Reports, vol. 149, Ocean Drill. Program, College Station, Tex.

Schärer, U., J. Girardeau, G. Cornen, and G. Boillot (2000), 138–121 Ma asthenospheric magmatism prior to continental break-up in the North Atlantic and geodynamic implications, *Earth Planet. Sci. Lett.*, *181*, 555–572.

Schettino, A., and C. Scotese (2002), Global kinematic constraints to the tectonic history of the Mediterranean region and surrounding areas during the Jurassic and Cretaceous, *J. Virtual Explor.*, *8*, 149–168.

Seipold, U., and F. R. Schilling (2003), Heat transport in serpentinites, *Tectonophysics*, *370*, 147–162.

Sibuet, J. C., et al. (1979), *Initial Reports of the Deep Sea Drilling Project*, vol. 47, 787 pp., U.S. Govt. Print. Off., Washington, D. C.

Souriau, A. (1984), Geoid anomalies over Gorringe Ridge, North Atlantic Ocean, *Earth Planet. Sci. Lett.*, *68*, 101–114.

Srivastava, S. P., W. R. Roest, L. C. Kovacs, G. Oakey, S. Lévesque, J. Verhoef, and R. Macnab (1990), Motion of the Iberia since the Late Jurassic: Results from detailed aeromagnetic measurements in the Newfoundland Basin, *Tectonophysics*, *184*, 229–260.

Stampfli, G. M., and G. D. Borel (2002), A plate tectonic model for the Paleozoic and Mesozoic constrained by dynamic plate boundaries and restored synthetic oceanic isochrons, *Earth Planet. Sci. Lett.*, *196*, 17–33.

Teixell, A., P. Ayarza, H. Zeyen, M. Fernàndez, and M. L. Arboleya (2005), Effects of mantle upwelling in a compressional setting: The Atlas Mountains of Morocco, *Terra Nova*, *17*, 456–461.

Terrinha, P., et al. (2003), Tsunamigenic-seismogenic structures, neotectonics, sedimentary processes and slope instability on the southwest Portuguese Margin, *Mar. Geol.*, *195*, 55–73.

Tortella, D., M. Torné, and A. Pérez-Estaún (1997), Geodynamic evolution of the eastern segment of the Azores-Gibraltar Zone: The Gorringe Bank and the Gulf of Cadiz region, *Mar. Geophys. Res.*, *19*, 211–230.

Ulmer, P., and V. Trommsdorff (1995), Serpentine stability to mantle depths and subduction-related magmatism, *Science*, *268*, 858–861.

Vergés, J., M. Fernàndez, and A. Martínez (2002), The Pyrenean orogen: Pre-, syn-, and post-collisional evolution, *J. Virtual Explor.*, *8*, 55–84.

Verzhbitsky, E. V., and V. G. Zolotarev (1989), Heat flow and the Eurasian-African plate boundary in the eastern part of the Azores-Gibraltar fracture zone, *J. Geod.*, *11*, 267–273.

Watts, A. B. (2001), *Isostasy and Flexure of the Lithosphere*, 458 pp., Cambridge Univ. Press, New York.

Whitmarsh, R. B., et al. (1998), *Proceedings of the Ocean Drilling Program: Initial Reports*, vol. 173, Ocean Drill. Program, College Station, Tex.

Zeyen, H., and M. Fernàndez (1994), Integrated lithospheric modeling combining thermal, gravity, and local isostasy analysis: Application to the NE Spanish Geotransect, *J. Geophys. Res.*, *99*(B9), 18,089–18,102.

Zeyen, H., P. Ayarza, M. Fernàndez, and A. Rimi (2005), Lithospheric structure under the western African-European plate boundary: A transect across the Atlas Mountains and the Gulf of Cadiz, *Tectonics*, *24*, TC2001, doi:10.1029/2004TC001639.

Zitellini, N., M. Rovere, P. Terrinha, F. Chierici, L. Matias, and Bigsets Team (2004), Neogene through Quaternary tectonic reactivation of SW Iberian passive margin, *Pure Appl. Geophys.*, *161*, 565–587, doi:510.1007/s00024-00003-02463-00024.

Zitellini, N., et al. (2009), The quest for the Africa-Eurasia plate boundary west of the Strait of Gibraltar, *Earth Planet. Sci. Lett.*, *280*, 13–50.

J. C. Afonso, ARC National Key Centre for Geochemical Evolution and Metallogeny of Continents, Department of Earth and Planetary Sciences, Macquarie University, NSW 2109, Sydney, Australia.

M. Fernàndez, D. Garcia-Castellanos, I. Jiménez-Munt, and J. Vergés, Group of Dynamics of the Lithosphere, Institute of Earth Sciences Jaume Almera, CSIC, Solé i Sabarís s/n, E-08028 Barcelona, Spain. (ivone@ija.csic.es)

J. Fullea, Geophysics Section, School of Cosmic Physics, Dublin Institute for Advanced Studies, 5 Merrion Square, Dublin 2, Ireland.